Technical University of Denmark

DTU

Results of the AVATAR project for the validation of 2D aerodynamic models with experimental data of the DU95W180 airfoil with unsteady flap

Ferreira, C.; Gonzalez, A.; Baldacchino, D.; Aparicio, M.; Gomez, S.; Munduate, X.; Ramos García, Néstor; Sørensen, Jens Nørkær; Jost, E.; Knecht, S.; Lutz, T.; Chassapogiannis, P.; Diakakis, K.; Papadakis, G.; Voutsinas, S.; Prospathopoulos, J.; Gillebaart, T.; van Zuijlen, A.

DTU Library
Technical Information Center of Denmark

Results of the AVATAR project for the validation of 2D aerodynamic models with experimental data of the DU95W180 airfoil with unsteady flap

Results of the AVATAR project for the validation of 2D aerodynamic models with experimental data of the DU95W180 airfoil with unsteady flap

C. Ferreira[1], A. Gonzalez[2], D. Baldacchino[1], M. Aparicio[2], S. Gómez[2], X. Munduate[2], N.R. Garcia[3], J.N. Sørensen, E. Jost[4], S. Knecht[4], T. Lutz[4], P. Chassapogiannis[5], K. Diakakis[5], G. Papadakis [5], S. Voutsinas[5], J. Prospathopoulos[5], T. Gillebaart[1], A. van Zuijlen[1]

[1]DUWIND, Faculty of Aerospace Engineering, Delft University of Technology, Kluyverweg 1, 2629HS Delft, The Netherlands
[2]CENER - National Renewable Energy Centre, Ciudad de la Innovación 7, Sarriguren, Navarra, 31621, Spain
[3]Technical University of Denmark, Department of Wind Energy, RisøCampus, Frederiksborgvej 399, 4000 Roskilde Denmark
[4]Institute of Aerodynamics and Gas Dynamics (IAG), University of Stuttgart, Pfaffenwaldring 21 Stuttgart 70569, Germany
[5]Laboratory of Aerodynamics, National Technical University of Athens, Greece

E-mail: `c.j.simaoferreira@tudelft.nl`

Abstract. The *FP7 AdVanced Aerodynamic Tools for lArge Rotors - Avatar* project aims to develop and validate advanced aerodynamic models, to be used in integral design codes for the next generation of large scale wind turbines (10-20MW). One of the approaches towards reaching rotors for 10-20MW size is the application of flow control devices, such as flaps. In *Task 3.2: Development of aerodynamic codes for modelling of flow devices on aerofoils and rotors* of the Avatar project, aerodynamic codes are benchmarked and validated against the experimental data of a DU95W180 airfoil in steady and unsteady flow, for different angle of attack and flap settings, including unsteady oscillatory trailing-edge-flap motion, carried out within the framework of *WP3: Models for Flow Devices and Flow Control, Task 3.1: CFD and Experimental Database*. The aerodynamics codes are: AdaptFoil2D, Foil2W, FLOWer, MaPFlow, OpenFOAM, Q³UIC, ATEFlap . The codes include unsteady Eulerian CFD simulations with grid deformation, panel models and indicial engineering models. The validation cases correspond to 18 steady flow cases, and 42 unsteady flow cases, for varying angle of attack, flap deflection and reduced frequency, with free and forced transition. The validation of the models show varying degrees of agreement, varying between models and flow cases.

1. Introduction

The pursuit for lower Cost of Energy (CoE) for wind turbines has resulted in new concepts with active and passive flow control devices ([1]). Most designs focus on increasing the control authority by either passively or actively changing the boundary conditions at the aerodynamic surface. Pre-bend blades, bend-twist coupled blades and vortex generators are examples of passive-control designs. For active control, most concepts involve local devices: microtabs,

boundary layer control and trailing edge flaps. A review of different actively controlled smart rotor concepts was presented in [2], concluding that trailing edge flaps are among the most promising concepts. In the past years the research continued to further assess and understand the possibilities and mechanisms of trailing edge flaps. In [3], a detail study is presented for the application of flaps in a full rotor by looking at the controller and it's signal to noise ratio, multiple flap systems and sensor (strain gauges) placement. Model predictive control, a new control concept, has been studied both numerically ([4]) and experimentally ([5]) with promising results. The work by ([6]) studied the concept of controlling the flap based on a pressure difference over the airfoil at different chord-wise positions using potential flow. [7] studied the trailing edge flap concept experimentally to demonstrate, test and determine the potential of the concept. In [8], different control concepts using an aero-servo-elastic code based on CFD are evaluated. More recently, the work in [9] studied three state-of-the-art numerical models (Reynolds Averaged Navier Stokes, inviscid-viscid interaction model and a dynamic stall model) for a pitching and a flapping airfoil.

Unsteady experimental validation data is required to fully understand the capabilities/drawbacks of the different models. A thorough experimental study on the influence of the flap motion on the forces was performed in [10]. The FP7-UPWIND project also considered trailing edge flaps on wind turbine airfoils ([11]). One of the aims of the *FP7 AdVanced Aerodynamic Tools for lArge Rotors - Avatar* project is to generate reliable simulation models and software tools to include flow control concepts such as trailing edge flaps on large wind turbine blades. Important issues are to predict the aerodynamic implications of flow devices at sectional and blade level, and to develop and validate low/intermediate models to be included in aeroelastic simulations on wind turbines which use flow devices.

This paper presents the validation of seven numerical models against the collected data for measurements on a DU95W180 airfoil equipped with an actuated rigid trailing edge flap with 20% chord in steady and unsteady flow, for different angle of attack and flap settings, including unsteady oscillatory trailing-edge-flap motion, in free and forced laminar-turbulent transition. Different flap oscillation amplitudes and reduced frequencies are employed. The experiments were conducted in the Low Turbulence Wind Tunnel of Delft University of Technology with a model of $c = 0.6m$ chord at a Reynolds number of $Re \approx 1.0 \times 10^6$. Data includes lift, drag and moment coefficient and pressure distribution over the surface of the airfoil, for both steady and unsteady flow. The experimental campaign was carried out within the framework of *WP3: Models for Flow Devices and Flow Control, Task 3.1: CFD and Experimental Database* of the *FP7-AVATAR* project. A digital database of the experimental data is available. The description of the experiment and experimental results is presented in [12].

This work build upon the work presented in [13], which presents the main results of *Task 3.2: Development of aerodynamic codes for modelling of flow devices on aerofoils and rotors* of the Avatar project.

2. Methodology
Seven aerodynamics codes and models are evaluated in this study : AdaptFoil2D, Foil2W, FLOWer, MaPFlow, OpenFOAM, Q³UIC and ATEFlap. The codes include unsteady Eulerian CFD simulations with grid deformation, panel models and indicial engineering models. A description of the models is presented in [13]. Five of these models (Foil2W, FLOWer, MaPFlow, OpenFOAM, Q³UIC) are validated with steady flow cases, while six (AdaptFoil2D, Foil2W, FLOWer, OpenFOAM, Q³UIC and ATEFlap) are validated against unsteady flow cases.

The experimental validation database encompasses 60 cases: 18 steady and 42 unsteady, varying flap angle, angle of attack, free and forced transition, reduced frequency k^1 of the flap

---

[1] $k = \frac{\omega c}{2U_\infty}$, where ω is the frequency of oscillation and U_∞ is the unperturbed flow velocity.

Case UNST 35. Case UNST 41.
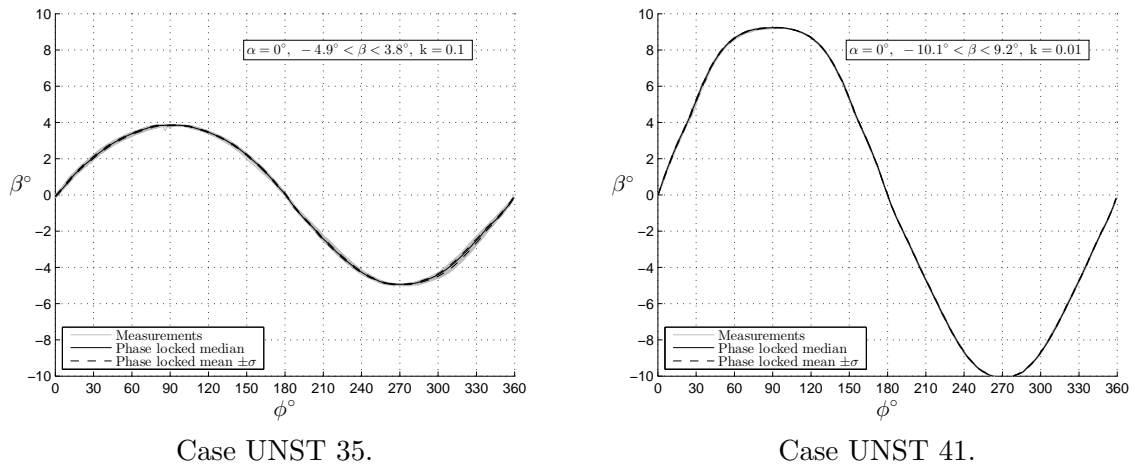
Figure 1. Example of the actuation of the flap angle β as a function of phase ϕ.

oscillation and amplitude of the oscillation. The list of unsteady cases are presented in Table 1.

In this report, we present the validation using integral load polars for both steady and unsteady cases. Due to the large set of results, only a limited subset of results is presented in this paper. Additionally, four validation terms are used: average lift coefficient for flap angle $\beta = 0°$, and amplitude between upstroke and downstroke values at $\beta = 0°$; and minimum and maximum lift coefficient during the cycle.

The actuation of the flap follow a quasi-sinusoidal shape, as shown by the experimental measurements of flap actuation for two of the cases (Figure 1).

3. Results and discussion
3.1. Results for steady cases
The steady flow cases are defined by the transition (free or forced, see [12]), angle of attack α (based on chord line with no flap deflection) and flap angle β. Figure 2 presents the steady polars for varying varying angle of attack, comparing lift, drag and moment coefficient[2] (C_l, C_d and C_m [3]) for the codes Foil2w, Q³UIC, OpenFOAM, FLOWer and MaPFlow, in free and forced transition. Figure 3 shows the comparison for the pressure distribution at $\beta = 9.2°$, for five angles of attack, in free and forced transition. The results show the validation with steady polars and pressure distributions for maximum flap deflection. The steady results for the case of $\beta = 9.2°$ show significant differences between the results from the models and the experimental results, in particular for the cases of forced transition. These differences are not only visible in terms of stall behaviour and post-stall, but also in the linear region of the lift curve. Differences in pressure distribution are mostly visible in the pressure side, in particular at the flap region.

3.2. Results for unsteady cases
Figure 4 presents an example of the validation of the numerical simulations with the unsteady experimental polars of the DU95W180 airfoil for in several configurations of varying flap angle and fixed angle of attack ($C_l - \beta$, $C_{d_p} - \beta$, $C_m - \beta$) at $Re \approx 1.0 * 10^6$, with free and forced transition. Although the angle of attack is low ($\alpha = 0°$), the results show significant differences in both average value and the hysteresis loop. These differences are more significant for the case of forced transition. With increasing angle of attack, these differences are more significant,

---

[2] At the quarter-chord position.
[3] Non-dimensioned by the unperturbed dynamic pressure and chord scale.

as seen by the results in Table 3. Table 3 shows the results for lift coefficient for unsteady test cases. Values indicate mean at flap angle $\beta = 0°$, and the difference between upstroke and downstroke values at flap angle $\beta = 0°$. Table 3 presents the results for maximum and minimum lift coefficient in the actuation cycle. Although all models capture the correct trends, the results show significant differences in mean value of the cycles and amplitude for the cases of larger angles of attack, and in particular for the cases of forced transition. These differences might arise not only of unsteady effects, but also from the uncertainty of the models in steady predictions, as seen in the previous section. In a comparison, the different models show similar order of magnitude of error in mean value of amplitude of the cycle; different models perform better for different cases.

4. Conclusions

The sub-set of results presented[4] shows that the difference between experimental and numerical results has two sources: an error in the prediction of average steady results; and an error in the prediction of unsteady flow effects. The results for attached flow ($\alpha = 0°$) show that the error in steady flow is also verified in unsteady flow; additionally, the difference in hysteresis amplitude at $\beta = 0°$ demonstrates an error in predicting unsteady effects. For regions of separated flow (or more dominant viscous effects), the models show differences in the estimation of the amplitude of the lift cycle, mostly by over-predicting lift in separated flow. A preliminary observation shows that the accuracy of the models compounds their accuracy in predicting steady loads (there is a small variation of error with reduced frequency) with the accuracy in predicting the hysteresis loop. For attached flow regions, these effects could perhaps be decoupled, providing two terms of validation and model improvement.

References

[1] Berg D E, Wilson D G, Resor B R, Barone M F, Berg J C, Kota S and Ervin G 2009 *Proc. of WindPower* 1–12
[2] Barlas T and van Kuik G 2010 *Progress in Aerospace Sciences* **46** 1–27 ISSN 03760421
[3] Andersen P B, Henriksen L, Gaunaa M, Bak C and Buhl T 2010 *Wind Energy* **13** 193–206 ISSN 10954244
[4] Barlas T K, Van Der Veen G J and Van Kuik G A M 2011 *Wind Energy* **15** 757–771 ISSN 10954244
[5] Castaignet D, Barlas T, Buhl T, Poulsen N K, Wedel-Heinen J J, Olesen N A, Bak C and Kim T 2013 *Wind Energy* **17** 549–564 ISSN 10991824
[6] Gaunaa M and Andersen P B 2009 *EWEC*
[7] Bak C, Gaunaa M, Andersen P B, Buhl T, Hansen P and Clemmensen K 2010 *Wind Energy* **13** 207–219
[8] Heinz J, Sørensen N N and Zahle F 2011 *Wind Energy* **14** 449–462 ISSN 10954244
[9] Bergami L, Riziotis V A and Gaunaa M 2014 *Wind Energy* ISSN 10954244
[10] Baek P, Jérémiaz J G, Kramer P and Gaunaa M 2011 *EWEA conference* 1–8
[11] Lutz T W A W W and Jeremiasz J 2011 Design and verification of an airfoil with trailing-edge flap and unsteady wind-tunnel tests Upwind wp1b3
[12] Ferreira C S, Baldacchino D, Ragni D, Bernardy S, Timmer N, Gillebaart T and Dedeic A 2015 Unsteady measurements of the du95w180 airfoil with oscillating flap report for task 3.1, FP7 - Avatar project
[13] Ferreira C, Gonzalez A, Baldacchino D, Aparicio M, Gómez S, X M, Barlas A, R G N, Sorensen N N, Troldborg N, Barakos G, Jost E, Knecht S, Lutz T, Chassapoyiannis P, Diakakis K, Manolesos M, Voutsinas S, Prospathopoulos J, Gillebaart T, Florentie L, van Zuijlen A and Reijerkerk M 2015 Task 3.2 : Development of aerodynamic codes for modelling of flow devices on aerofoils and rotors report for task 3.2, FP7 - Avatar project

[4] A limited set of results is presented due to paper-length limit. A more complete analysis if planned for a future publication.

					Codes					
Case	Transition	α (°)	β (°)	k	Q³UIC	FoiL2W	FLOWer	AdapFoil2D	OpenFOAM	ATEFlap
UNST 1	free	0	$-5.0:3.9$	0.01	✓✓	✓✓		✓		
UNST 2	forced	0	$-5.0:3.9$	0.01		✓✓	✓✓		✓	✓
UNST 3	free	0	$-5.0:3.9$	0.05	✓✓	✓✓		✓		
UNST 4	forced	0	$-5.0:3.9$	0.05		✓✓	✓✓		✓	✓
UNST 5	free	0	$-4.9:3.9$	0.1	✓✓	✓✓		✓		
UNST 6	forced	0	$-4.9:3.9$	0.1		✓✓	✓✓		✓	✓
UNST 7	free	0	$-10.1:9.2$	0.01	✓✓	✓✓		✓		
UNST 8	forced	0	$-10.1:9.2$	0.01		✓✓	✓✓		✓	✓
UNST 9	free	0	$-10.1:9.2$	0.05	✓✓	✓✓		✓		
UNST 10	forced	0	$-10.1:9.2$	0.05		✓✓	✓✓		✓	✓
UNST 11	free	0	$-10.0:9.2$	0.1	✓✓	✓✓		✓		
UNST 12	forced	0	$-10.0:9.2$	0.1		✓✓	✓✓		✓	✓
UNST 13	free	8	$-5.0:3.9$	0.01	✓✓	✓✓		✓		
UNST 14	forced	8	$-5.0:3.9$	0.01		✓✓	✓✓		✓	✓
UNST 15	free	8	$-5.0:3.9$	0.05	✓✓	✓✓		✓		
UNST 16	forced	8	$-5.0:3.9$	0.05		✓✓	✓✓		✓	✓
UNST 17	free	8	$-4.9:3.9$	0.1	✓✓	✓✓		✓		
UNST 18	forced	8	$-4.9:3.9$	0.1		✓✓	✓✓		✓	✓
UNST 19	free	8	$-10.1:9.2$	0.01	✓✓	✓✓		✓		
UNST 20	forced	8	$-10.1:9.2$	0.01		✓✓	✓✓		✓	✓
UNST 21	free	8	$-10.0:9.2$	0.05	✓✓	✓✓		✓		
UNST 22	forced	8	$-10.1:9.2$	0.05		✓✓	✓✓		✓	✓
UNST 23	free	8	$-10.0:9.2$	0.1	✓✓	✓✓		✓		
UNST 24	forced	8	$-10.0:9.2$	0.1		✓✓	✓✓		✓	✓
UNST 25	free	10	$-5.0:3.9$	0.01	✓✓	✓✓		✓		
UNST 26	free	10	$-5.0:3.9$	0.05	✓✓	✓✓		✓		
UNST 27	free	10	$-4.9:3.9$	0.1	✓✓	✓✓		✓		
UNST 28	free	10	$-10.1:9.2$	0.01		✓✓		✓		
UNST 29	free	10	$-10.1:9.2$	0.05		✓✓		✓		
UNST 30	free	10	$-10.0:9.2$	0.1		✓✓		✓		
UNST 31	free	18	$-5.0:3.8$	0.01		✓✓		✓		
UNST 32	forced	18	$-5.0:3.9$	0.01		✓✓			✓	✓
UNST 33	free	18	$-5.0:3.8$	0.05		✓✓		✓		
UNST 34	forced	18	$-4.9:3.9$	0.05		✓✓			✓	✓
UNST 35	free	18	$-4.9:3.8$	0.1		✓✓		✓		
UNST 36	forced	18	$-4.9:3.9$	0.1		✓✓			✓	✓
UNST 37	free	18	$-10.1:9.2$	0.01		✓✓		✓		
UNST 38	forced	18	$-10.1:9.2$	0.01		✓✓				
UNST 39	free	18	$-10.1:9.2$	0.05		✓✓		✓		
UNST 40	forced	18	$-10.1:9.2$	0.05		✓✓			✓	✓
UNST 41	free	18	$-10.0:9.2$	0.1		✓✓		✓		
UNST 42	forced	18	$-10.0:9.2$	0.1		✓✓			✓	✓

Legend:

✓: validation through polars $C_l - \beta$, $C_{d_p} - \beta$ and $C_m - \beta$.

✓✓: validation includes unsteady pressure distribution.

Table 1. Unsteady test cases used for the validation of the different codes. All cases at chord based Reynolds number $Re \approx 1.0 * 10^6$.
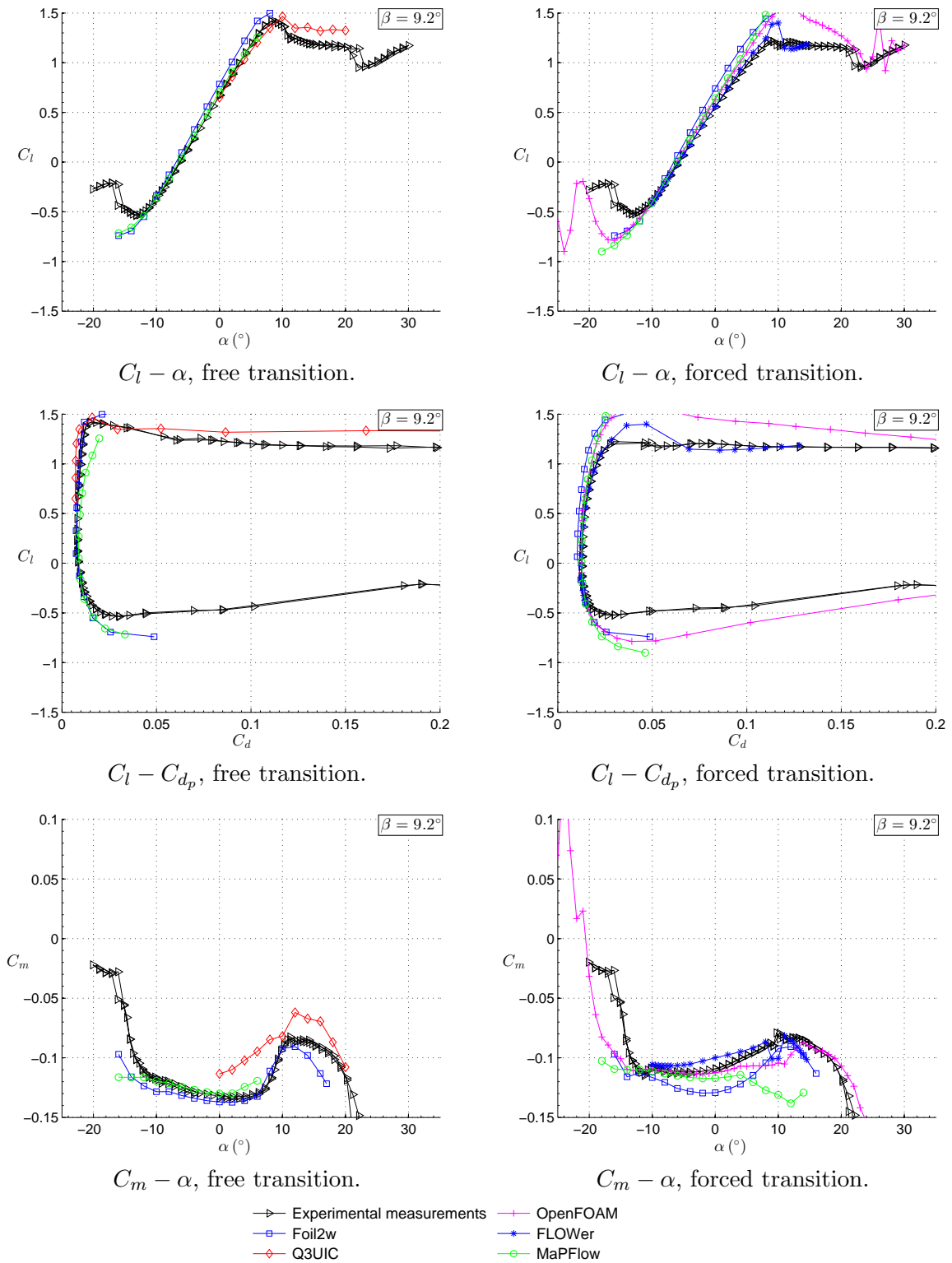
Figure 2. Validation of the numerical simulations with the steady experimental polars of the DU95W180 airfoil for varying angle of attack and fixed flap angle ($C_l - \alpha$, $C_l - C_d$, $C_m - \alpha$) at $Re \approx 1.0 * 10^6$, with free and forced transition, for $\beta = 9.2°$ and $-20° < \alpha < 30°$ (cases STDY5 and STDY10).
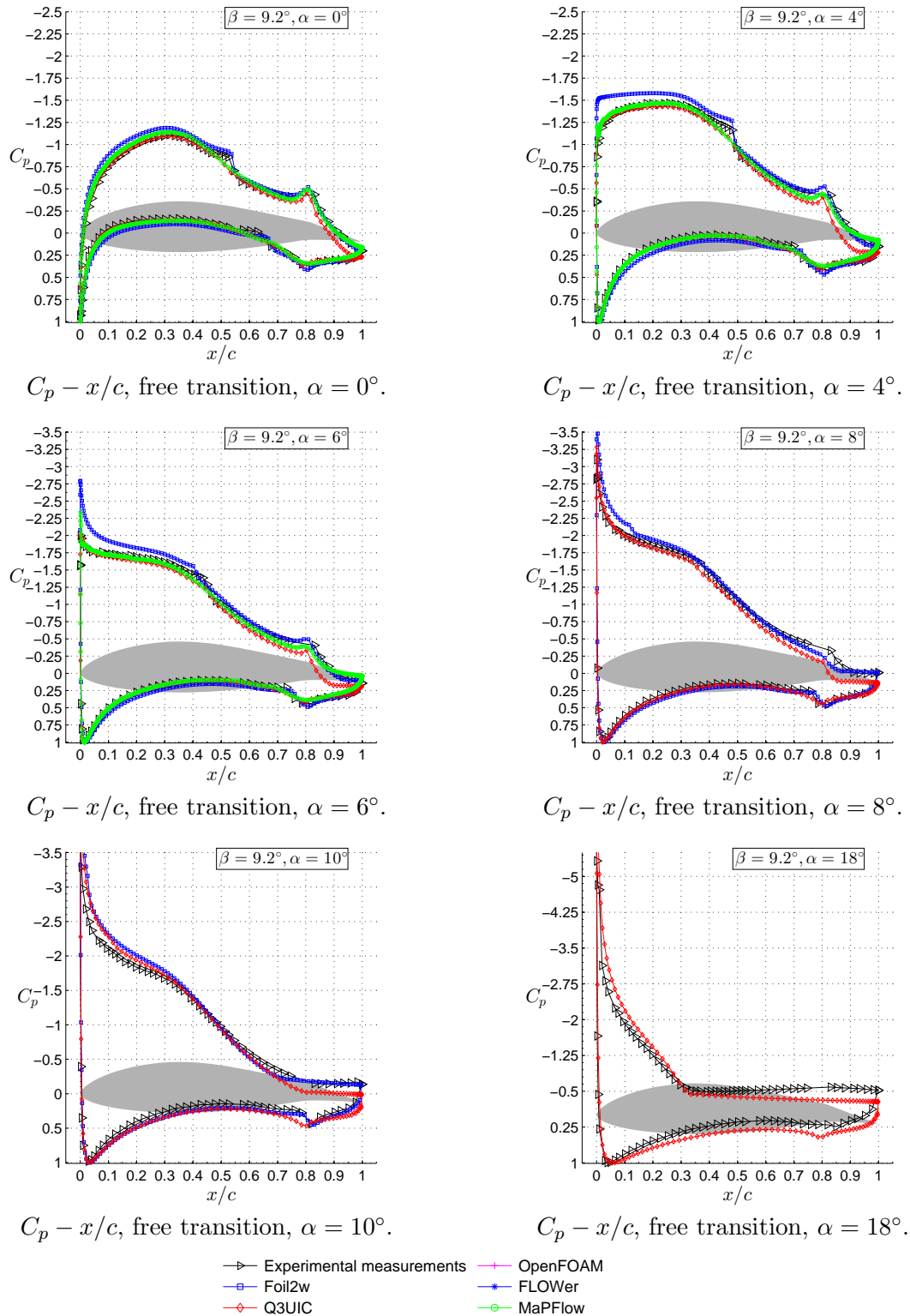
Figure 3. Validation of the numerical simulations with the steady experimental pressure distribution of the DU95W180 airfoil for several angle of attacks and flap angle $\beta = 9.2°$, at $Re \approx 1.0 * 10^6$, with free transition (case STDY5).
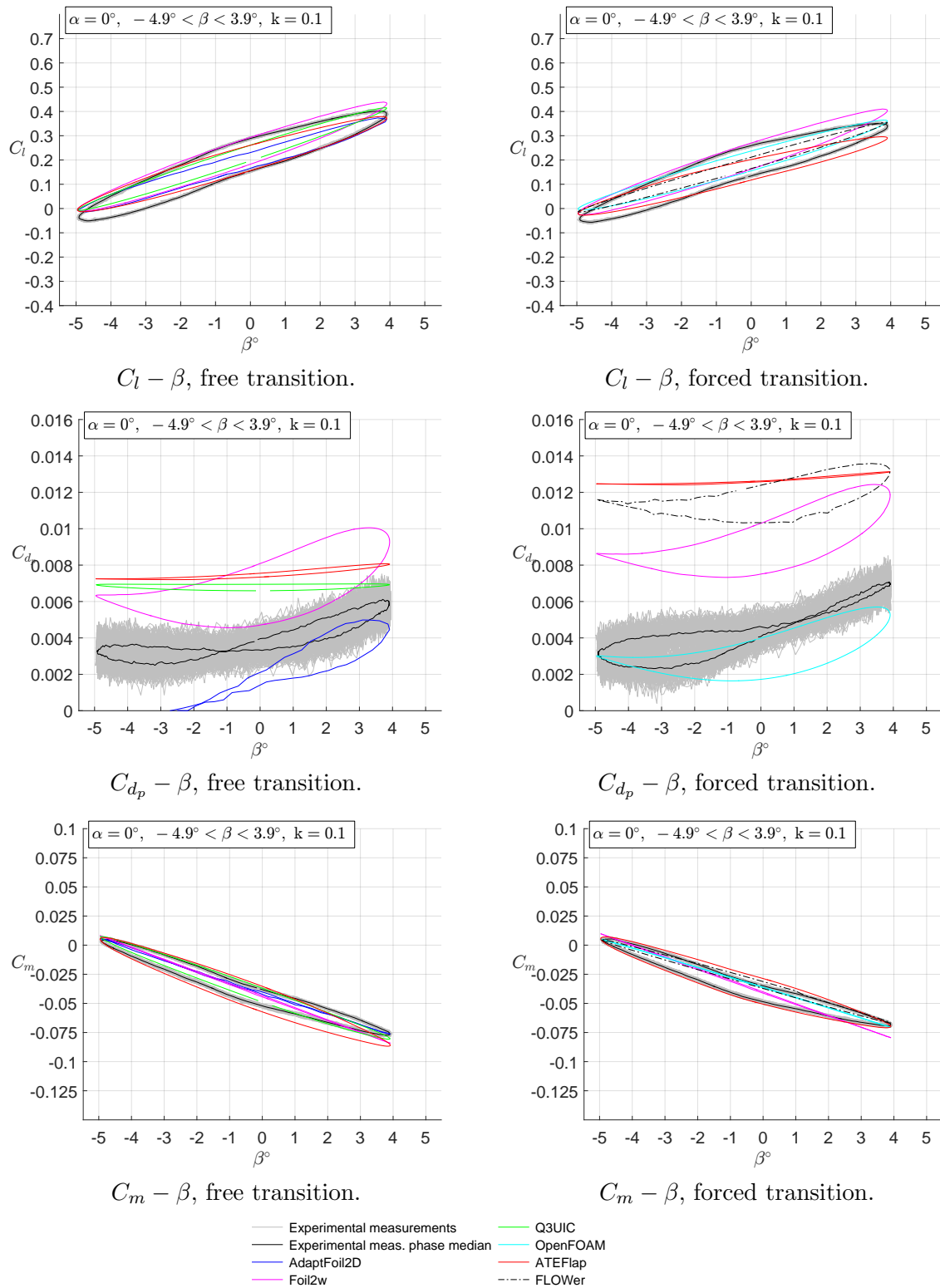
Figure 4. Validation of the numerical simulations with the unsteady experimental polars of the DU95W180 airfoil for varying flap angle and fixed angle of attack ($C_l - \beta$, $C_{d_p} - \beta$, $C_m - \beta$) at $Re \approx 1.0 * 10^6$, with free and forced transition, for $\alpha = 0°$, $-4.9° < \beta < 3.9°$, $k = 0.1$ (cases UNST5 and UNST6).

		Codes					
Case	Experimental	Q³UIC	FoiL2W	FLOWer	AdapFoil2D	OpenFOAM	ATEFlap
UNST 1	0.23 ⁊ 0.025	0.00 ⁊ -0.008	0.01 ⁊ 0.007		-0.04 ⁊ -0.009		-0.02 ⁊ 0.005
UNST 2	0.19 ⁊ 0.018		0.03 ⁊ 0.013	-0.00 ⁊ -0.009		0.00 ⁊ 0.005	-0.03 ⁊ 0.006
UNST 3	0.23 ⁊ 0.087	0.00 ⁊ -0.032	0.01 ⁊ 0.001		-0.02 ⁊ -0.044		-0.01 ⁊ 0.004
UNST 4	0.19 ⁊ 0.065		0.02 ⁊ 0.020	-0.00 ⁊ -0.031		0.00 ⁊ -0.001	-0.03 ⁊ 0.008
UNST 5	0.22 ⁊ 0.134	0.01 ⁊ -0.070	0.02 ⁊ -0.024		-0.02 ⁊ -0.070		-0.01 ⁊ -0.030
UNST 6	0.20 ⁊ 0.125		0.02 ⁊ -0.017	-0.01 ⁊ -0.078		-0.00 ⁊ -0.043	-0.04 ⁊ -0.041
UNST 7	0.23 ⁊ 0.044	0.01 ⁊ -0.010	0.01 ⁊ 0.023		-0.03 ⁊ -0.020		-0.01 ⁊ 0.019
UNST 8	0.19 ⁊ 0.034		0.03 ⁊ 0.030	-0.01 ⁊ -0.026		0.01 ⁊ 0.013	-0.03 ⁊ 0.016
UNST 9	0.23 ⁊ 0.182	0.01 ⁊ -0.066	0.02 ⁊ 0.007		-0.04 ⁊ -0.062		-0.01 ⁊ 0.017
UNST 10	0.20 ⁊ 0.141		0.02 ⁊ 0.043	-0.01 ⁊ -0.095		0.00 ⁊ -0.007	-0.04 ⁊ 0.022
UNST 11	0.22 ⁊ 0.290	0.01 ⁊ -0.147	0.02 ⁊ -0.046		-0.04 ⁊ -0.125		-0.01 ⁊ -0.056
UNST 12	0.19 ⁊ 0.232		0.03 ⁊ 0.006	-0.01 ⁊ -0.151		0.01 ⁊ -0.058	-0.03 ⁊ -0.041
UNST 13	1.10 ⁊ 0.012	0.01 ⁊ -0.002	0.06 ⁊ 0.016		-0.07 ⁊ 0.005		-0.04 ⁊ 0.017
UNST 14	0.91 ⁊ 0.001		0.18 ⁊ 0.019	0.04 ⁊ 0.004		0.09 ⁊ 0.014	-0.03 ⁊ 0.002
UNST 15	1.10 ⁊ 0.066	0.01 ⁊ -0.037	0.07 ⁊ 0.012		-0.06 ⁊ -0.004		-0.04 ⁊ 0.007
UNST 16	0.91 ⁊ 0.011		0.18 ⁊ 0.051	0.04 ⁊ 0.003		0.09 ⁊ 0.032	-0.03 ⁊ 0.001
UNST 17	1.09 ⁊ 0.108	0.01 ⁊ -0.081	0.07 ⁊ -0.006		-0.06 ⁊ -0.024		-0.04 ⁊ -0.026
UNST 18	0.90 ⁊ 0.035		0.18 ⁊ 0.051	0.04 ⁊ -0.010		0.09 ⁊ 0.025	-0.03 ⁊ -0.020
UNST 19	1.10 ⁊ 0.023	0.01 ⁊ -0.005	0.06 ⁊ 0.035		-0.06 ⁊ 0.015		-0.04 ⁊ 0.031
UNST 20	0.91 ⁊ 0.001		0.18 ⁊ 0.043	0.03 ⁊ 0.024		0.09 ⁊ 0.029	-0.03 ⁊ 0.008
UNST 21	1.09 ⁊ 0.136	0.00 ⁊ -0.100	0.06 ⁊ 0.020		-0.05 ⁊ 0.017		-0.05 ⁊ 0.010
UNST 22	0.90 ⁊ 0.037		0.18 ⁊ 0.099	0.04 ⁊ 0.006		0.09 ⁊ 0.053	-0.03 ⁊ 0.013
UNST 23	1.07 ⁊ 0.219	0.01 ⁊ -0.201	0.08 ⁊ -0.015		-0.03 ⁊ 0.006		-0.03 ⁊ -0.049
UNST 24	0.89 ⁊ 0.127		0.18 ⁊ 0.061	0.04 ⁊ -0.063		0.09 ⁊ -0.005	-0.02 ⁊ -0.068
UNST 25	1.21 ⁊ 0.007	-0.02 ⁊ 0.011	0.07 ⁊ -0.006		0.02 ⁊ 0.001		
UNST 26	1.21 ⁊ 0.007	-0.01 ⁊ 0.048	0.07 ⁊ -0.004		0.02 ⁊ 0.001		
UNST 27	1.21 ⁊ 0.016	-0.01 ⁊ 0.069	0.07 ⁊ -0.009		0.04 ⁊ 0.016		
UNST 28	1.21 ⁊ 0.018		0.06 ⁊ -0.015		0.03 ⁊ -0.016		
UNST 29	1.20 ⁊ 0.020		0.07 ⁊ -0.009		0.06 ⁊ 0.091		
UNST 30	1.16 ⁊ 0.006		0.11 ⁊ 0.058		0.08 ⁊ 0.144		
UNST 31	1.02 ⁊ 0.019		0.35 ⁊ -0.007		0.20 ⁊ -0.013		-0.04 ⁊ -0.006
UNST 32	1.02 ⁊ 0.007		0.35 ⁊ 0.005			0.15 ⁊ 0.041	-0.04 ⁊ 0.001
UNST 33	1.03 ⁊ 0.028		0.37 ⁊ 0.003		0.19 ⁊ -0.003		-0.06 ⁊ 0.027
UNST 34	1.02 ⁊ 0.014		0.38 ⁊ 0.017			0.17 ⁊ 0.001	-0.03 ⁊ 0.036
UNST 35	1.03 ⁊ 0.043		0.37 ⁊ -0.031		0.22 ⁊ -0.022		-0.06 ⁊ 0.024
UNST 36	1.02 ⁊ 0.042		0.38 ⁊ -0.030			0.17 ⁊ -0.039	-0.03 ⁊ 0.022
UNST 37	1.03 ⁊ 0.029		0.33 ⁊ -0.008		0.17 ⁊ -0.012		-0.06 ⁊ 0.003
UNST 38	1.02 ⁊ 0.035		0.35 ⁊ -0.015			0.15 ⁊ 0.009	-0.04 ⁊ -0.011
UNST 39	1.03 ⁊ 0.033		0.34 ⁊ 0.024		0.21 ⁊ -0.026		-0.08 ⁊ 0.076
UNST 40	1.02 ⁊ 0.036		0.35 ⁊ 0.022			0.16 ⁊ -0.028	-0.04 ⁊ 0.098
UNST 41	1.03 ⁊ 0.077		0.35 ⁊ -0.061		0.23 ⁊ -0.045		-0.08 ⁊ 0.052
UNST 42	1.02 ⁊ 0.066		0.37 ⁊ -0.049			0.17 ⁊ -0.052	-0.03 ⁊ 0.106

Table 2. Results for lift coefficient for unsteady test cases. Values indicate mean at flap angle $\beta = 0°$, ⁊ difference between upstroke and downstroke values at flap angle $\beta = 0°$. Values for *Experimental* are absolute, values for *Codes* are relative to *Experimental* (difference to).

| | | Codes | | | | | |
Case	Experimental	Q³UIC	FoiL2W	FLOWer	AdapFoil2D	OpenFOAM	ATEFlap
UNST 1	-0.071 ⁊ 0.427	0.025 ⁊ 0.018	0.009 ⁊ 0.053		0.014 ⁊ -0.015		0.003 ⁊ -0.004
UNST 2	-0.074 ⁊ 0.372		-0.001 ⁊ 0.077	0.039 ⁊ -0.000		0.031 ⁊ 0.023	-0.001 ⁊ -0.041
UNST 3	-0.065 ⁊ 0.418	0.036 ⁊ 0.015	0.027 ⁊ 0.043		0.030 ⁊ -0.023		0.027 ⁊ -0.018
UNST 4	-0.068 ⁊ 0.365		0.016 ⁊ 0.067	0.043 ⁊ 0.001		0.043 ⁊ 0.017	0.019 ⁊ -0.052
UNST 5	-0.051 ⁊ 0.401	0.042 ⁊ 0.015	0.040 ⁊ 0.038		0.037 ⁊ -0.027		0.038 ⁊ -0.022
UNST 6	-0.057 ⁊ 0.350		0.031 ⁊ 0.060	0.042 ⁊ 0.005		0.051 ⁊ 0.014	0.029 ⁊ -0.054
UNST 7	-0.340 ⁊ 0.707	0.023 ⁊ -0.057	-0.034 ⁊ 0.070		-0.048 ⁊ -0.057		0.003 ⁊ -0.050
UNST 8	-0.347 ⁊ 0.605		-0.032 ⁊ 0.128	0.094 ⁊ -0.021		0.071 ⁊ 0.024	0.111 ⁊ -0.058
UNST 9	-0.328 ⁊ 0.690	0.037 ⁊ -0.040	0.002 ⁊ 0.054		-0.017 ⁊ -0.078		0.030 ⁊ -0.066
UNST 10	-0.331 ⁊ 0.595		-0.002 ⁊ 0.108	0.095 ⁊ -0.015		0.088 ⁊ 0.013	0.097 ⁊ -0.080
UNST 11	-0.297 ⁊ 0.657	0.041 ⁊ -0.014	0.022 ⁊ 0.045		0.008 ⁊ -0.089		0.051 ⁊ -0.070
UNST 12	-0.302 ⁊ 0.572		0.018 ⁊ 0.091	0.087 ⁊ -0.019		0.095 ⁊ 0.009	0.101 ⁊ -0.091
UNST 13	0.816 ⁊ 1.263	0.039 ⁊ -0.032	0.047 ⁊ 0.094		-0.060 ⁊ -0.041		-0.034 ⁊ -0.040
UNST 14	0.704 ⁊ 1.018		0.119 ⁊ 0.238	0.055 ⁊ 0.051		0.070 ⁊ 0.138	-0.009 ⁊ -0.052
UNST 15	0.818 ⁊ 1.259	0.051 ⁊ -0.027	0.067 ⁊ 0.091		-0.044 ⁊ -0.046		-0.007 ⁊ -0.044
UNST 16	0.705 ⁊ 1.020		0.138 ⁊ 0.228	0.060 ⁊ 0.049		0.084 ⁊ 0.129	0.006 ⁊ -0.062
UNST 17	0.832 ⁊ 1.249	0.053 ⁊ -0.014	0.080 ⁊ 0.088		-0.029 ⁊ -0.056		0.004 ⁊ -0.042
UNST 18	0.707 ⁊ 1.023		0.159 ⁊ 0.213	0.065 ⁊ 0.041		0.098 ⁊ 0.116	0.014 ⁊ -0.066
UNST 19	0.546 ⁊ 1.413	0.034 ⁊ -0.075	-0.012 ⁊ 0.076		-0.039 ⁊ 0.004		-0.224 ⁊ -0.079
UNST 20	0.488 ⁊ 1.172		0.029 ⁊ 0.253	0.058 ⁊ 0.062		0.049 ⁊ 0.162	-0.091 ⁊ -0.118
UNST 21	0.557 ⁊ 1.415	0.049 ⁊ -0.073	0.025 ⁊ 0.084		-0.010 ⁊ 0.010		-0.025 ⁊ -0.070
UNST 22	0.493 ⁊ 1.173		0.068 ⁊ 0.248	0.065 ⁊ 0.053		0.074 ⁊ 0.150	0.044 ⁊ -0.122
UNST 23	0.587 ⁊ 1.419	0.052 ⁊ -0.057	0.049 ⁊ 0.081		0.004 ⁊ -0.032		0.001 ⁊ -0.071
UNST 24	0.507 ⁊ 1.178		0.108 ⁊ 0.232	0.072 ⁊ 0.044		0.096 ⁊ 0.131	0.057 ⁊ -0.120
UNST 25	1.017 ⁊ 1.270	0.027 ⁊ 0.039	0.053 ⁊ 0.130		-0.022 ⁊ 0.105		
UNST 26	1.017 ⁊ 1.270	0.030 ⁊ 0.041	0.063 ⁊ 0.137		-0.022 ⁊ 0.105		
UNST 27	1.019 ⁊ 1.275	-0.027 ⁊ 0.041	0.068 ⁊ 0.140		-0.011 ⁊ 0.105		
UNST 28	0.773 ⁊ 1.351		-0.013 ⁊ 0.143		-0.024 ⁊ 0.128		
UNST 29	0.782 ⁊ 1.359		0.017 ⁊ 0.172		-0.005 ⁊ 0.113		
UNST 30	0.801 ⁊ 1.400		0.036 ⁊ 0.151		0.019 ⁊ 0.083		
UNST 31	0.914 ⁊ 1.101		0.356 ⁊ 0.315		0.244 ⁊ 0.185		0.013 ⁊ -0.111
UNST 32	0.904 ⁊ 1.090		0.380 ⁊ 0.330			0.137 ⁊ 0.208	0.047 ⁊ -0.094
UNST 33	0.925 ⁊ 1.084		0.333 ⁊ 0.384		0.224 ⁊ 0.217		-0.003 ⁊ -0.076
UNST 34	0.910 ⁊ 1.079		0.362 ⁊ 0.392			0.143 ⁊ 0.220	0.034 ⁊ -0.065
UNST 35	0.918 ⁊ 1.091		0.317 ⁊ 0.401		0.227 ⁊ 0.237		-0.006 ⁊ -0.068
UNST 36	0.908 ⁊ 1.082		0.340 ⁊ 0.413			0.148 ⁊ 0.213	0.021 ⁊ -0.053
UNST 37	0.822 ⁊ 1.181		0.315 ⁊ 0.254		0.217 ⁊ 0.210		-0.185 ⁊ -0.184
UNST 38	0.803 ⁊ 1.175		0.340 ⁊ 0.259			0.110 ⁊ 0.369	-0.111 ⁊ -0.174
UNST 39	0.826 ⁊ 1.177		0.263 ⁊ 0.367		0.217 ⁊ 0.225		-0.015 ⁊ -0.137
UNST 40	0.792 ⁊ 1.160		0.303 ⁊ 0.384			0.114 ⁊ 0.229	0.111 ⁊ -0.103
UNST 41	0.821 ⁊ 1.187		0.206 ⁊ 0.405		0.241 ⁊ 0.239		0.008 ⁊ -0.108
UNST 42	0.793 ⁊ 1.168		0.237 ⁊ 0.424			0.109 ⁊ 0.220	0.072 ⁊ -0.073

Table 3. Results for lift coefficient for unsteady test cases. Values indicate minimum and maximum. Values for *Experimental* are absolute, values for *Codes* are relative to *Experimental* (difference to).